Experimental determination of statistical representative volume element in plane strain compression of dense sand

Volume Elémentaire Représentatif mesuré par la technologie d'analyse des images numériques au

E. R. Jang, C. K. Chung & M. M. Kim
Department of Civil & Environmental Engineering, Seoul National University, Korea
Y.-H. Jung
Department of Civil Engineering, Kyung Hee University, Korea

ABSTRACT
To appropriately account for wide variance of soil responses in computing averaged properties of granular soils, the representative volume element (RVE) of the soil specimen in plane strain experiment was investigated. A compression test on Jumunjin sand was conducted via the plain strain testing device with a transparent wall to capture the digital images without distortion. The displacement of a particular material point centered at a particle subset was measured via digital image analysis using two consecutive captured images. To evaluate engineering strains from the heterogeneous displacement field, we employed the linear regression of the displacement in the selected subset of an image. Various sizes of the RVE of the soil specimen were tested in terms of the statistics of the deformation modulus. Deformation modulus in a selected size of the particle subset was evaluated from the strain field obtained from the digital image analysis. By analyzing the statistics of the deformation moduli distribution for various sizes of the RVE, we discussed the proper size of the RVE of the soil specimen subject to the plane strain compression.

RÉSUMÉ
L'étude du Volume Elémentaire Représentatif (VER) a été effectuée sur l'échantillon du sol, au test de contraintes plantes, afin d'expliquer approximativement les réactions du sol à la fois vastes et variées dans le calcul des propriétés moyennes du sol granulaire. Afin de capturer les images numériques sans déformation, a été effectué l'essai de compression des sables de Jumunjin par le dispositif de test de contraintes planes doté d'un paroi transparent. Le déplacement d'un point matériel particulier centré à un sous-ensemble de particules a été mesuré par l'intermédiaire de l'analyse d'image numérique utilisant deux images saisies consécutives. Pour évaluer des contraintes technologiques du déplacement hétérogène mis en place, nous avons utilisé le linéaire du déplacement dans le sous-ensemble choisi d'une image. De diverses tailles du Volume Elémentaire Représentatif du spécimen du sol ont été examinées en termes de statistiques du coefficient élastique. Le coefficient élastique dans une taille choisie du sous-ensemble de particules a été évalué à partir du champ de contraintes obtenu par l'analyse d'images numériques. En analysant les statistiques des coefficients élastiques aussi bien que la distribution de contraintes pour les différentes tailles du Volume Elémentaire Représentatif, nous avons discuté la taille appropriée du Volume Elémentaire Représentatif du spécimen du présent sol à la compression de contrainte plate.

Keywords : representative volumen element (RVE), digital image analysis, particle image velocimetry (PIV), plane strain test

1 INTRODUCTION

From the viewpoint of micromechanics, it is inevitable that granular material, for example the cohesionless soil, has random heterogeneity due to its discrete nature. In practice, however, engineering analysis and design have been still based on homogeneous continuum mechanics in a large part of geotechnical and industrial application. This problem has been tackled firstly in the field of composite mechanics. Recently, a concept of the finite volume (Drugan and Willis 1996; Grufman and Ellyin 2007; Kanit et al. 2003; Trias et al. 2006) has been introduced to derive average properties of microscopically heterogeneous materials in a rational way. The finite volume is also known as the representative volume element (RVE) which satisfies the statistical homogeneity.

The RVE is usually regarded as a volume of the heterogeneous material which is sufficiently large to statistically represent every feature of micro-structural heterogeneities. However, the RVE should also be small enough to consider both various boundary conditions and many freedoms of deformation in continuum mechanics. According to Drugan and Willis (1996), the RVE can be defined as "the smallest material volume element for which the usual spatially constant overall modulus macroscopic constitutive representation is a sufficiently accurate model to represent mean constitutive response."

Comparing to the field of composite mechanics, soil mechanics rarely have dealt with particulate nature of granular materials. In recent years, the discrete element method, which explicitly simulates heterogeneous movement of discrete particles, has been reappraised because of the remarkable improvement of the computing power. Kruyt and Rothenburg (2001) and Wellmann et al. (2008) attempted to statistically analyze the heterogeneous response of granular soils based on the information from discrete element simulation. However, the experimental study of the representative volume element size has rarely been attempted.

Herein, we investigated statistics of the RVE size of granular soils. A plane strain compression test on Jumunjin sand was conducted. A plane strain testing apparatus, which is equipped with a special transparent wall to capture digital images without distortion, was used. The displacements at center points of selected particle subsets were measured via the digital image analysis using two images with a time interval taken during the test. To evaluate the engineering strains from the heterogeneous displacement field of particle subsets, we employed the linear regression on the displacement in unit elements, and subsequently differentiated the linear displacement field to obtain strains.

The statistics of the deformation moduli for various sizes of the observation window in the processed digital images was presented. The descriptive statistics provide the quantitative information to determine the optimum size of the RVE accounting for the microscopic heterogeneity in the overall deformation modulus.

Proceedings of the 17th International Conference on Soil Mechanics and Geotechnical Engineering
M. Hamza et al. (Eds.)

doi:10.3233/978-1-60750-031-5-466

2 PLANE STRAIN EXPERIMENT

2.1 *Testing Apparatus*

The apparatus uses a prismatic specimen with 128 mm height, 65 mm width and 45 mm length, surrounded by a top loading plate, a bottom plate and two side walls. Two lubricated side walls are connected with a fixed pedestal. To make sure the complete plane strain condition, two walls are braced with two horizontal bars to restrain relative movement of the side walls. For internal measurement, an earth pressure gauge is embedded in an aluminum side wall, and transparent acryl was chosen to manufacture the other side wall.

To simulate the frictionless condition at top and bottom ends, the bottom plate is free to move in one horizontal direction. This bottom plate is composed of two mechanical parts: the lower plate fixed on the pedestal and the upper plate moved freely on linear bearings between two plates. This mechanical composition allows for more efficient condition to track a shear band generation by minimizing the friction on end platens. The pressure cell with rectangular section was used to prevent the refraction of digital images, which occurs in the conventional cylindrical cells. Global measurement of the deformation of a specimen was made with the external LVDT and the load cell transducer.

2.2 *Testing condition and procedure*

The soil used in the study was Jumunjin sand, fine-grained quartz sand. Table 1 summarizes index properties of testing soil. Specimens were prepared by tamping dry sand in a rectangular mold. A specimen mounted between the side walls was flushed by CO_2 gas, and then de-aired water, and subsequently was saturated by applying back pressure of 100 kPa. Saturation was checked with B value of 0.95. To consolidate the specimen under K_0 condition, axial stress was applied while keeping the same magnitude of the confining pressure as the pressure measured on the side wall. Prior to plane strain compression, the axial effective stress reached 370 kPa, and the magnitude of the confining and wall stresses was 100 kPa.

In the plane strain condition, the specimen was compressed until the stress-strain response exhibits the residual state. During compression, sequential digital images, the size 2016 x 1512 pixels, of the transparent side wall were taken by a high-resolution digital camera.

Table 1. Index properties of the testing material

USUC	G_s	e_{max}	e_{min}	D_{50}	C_u	C_c	D_r
SP	2.65	0.992	0.596	0.56	1.53	0.94	74%

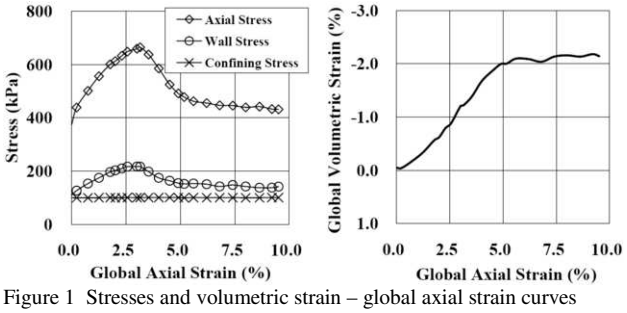

Figure 1 Stresses and volumetric strain – global axial strain curves

2.3 *Global stress-strain responses*

Figure 1 shows the results of global stress- strain responses. As shown in Figure 1, the peak axial stress is observed at the global axial strain ($(\varepsilon_a)_{global}$)of 3.15%, which corresponds to the friction angle of 44.20°. After exhibiting peak, the specimen kept continuously dilated until the global axial strain reaches 5.17%.

3 DIGITAL IMAGE ANALYSIS

Among the various technique of digital image analysis, two major techniques—Particle Image Velocimetry (PIV) and Digital Image Correlation (DIC)—have been widely used in deformation measurement in geotechnical testing (Rechenmacher and Finno 2004; White et al. 2003). Both techniques have the process in common; relative displacements are obtained from the correlation of pixel subsets by using two digital images taken at different times in a deformation process. However, they are different in details of processing algorithm; the DIC considers the deformation of a pixel subset in the target image, while the PIV regards a small part of the specimen as a rigid body. Herein, we employed the PIV in deformation measurement because of its goodness in convergence as well as the simplicity in the algorithm. To perform the image analysis, an object should be flat and deform within a plane of which the image is supposed to be taken. This requirement can easily be satisfied in the plane strain experiment.

To conduct the PIV, the center points and the size of pixel subsets in an initial digital image are selected. Let consider two consecutive images. The cross-correlation between a subset chosen in the initial image and the corresponding subset which is slightly shifted in the next image can be evaluated. The peak value of the correlation coefficient indicates that the shifted subset has the most similarity to the initial subset, thus the offset of two subsets indicates the displacement of the point at the center of the initial subset.

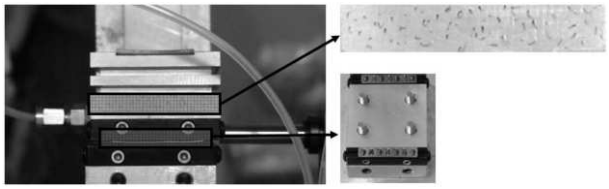

Figure 2. Random marks at movable bottom plate on linear bearings

Checking accuracy, precision and resolution is essential in use of the digital image analysis technique. To confirm full accuracy of the PIV, herein, a simple test was conducted. At first, we randomly marked 72 points on a movable plate with linear ball bearings at the bottom (see Figure 2). Digital still camera and light source were located right above the plate. Subsequently, the plate was horizontally shifted using the micrometer with 0.001-mm resolution, while sequential digital still images were captured. The accuracy of the PIV was checked by comparing the displacement of marked points obtained from the digital image analysis with reference displacement of the micrometer.

Table 2 summarizes the average displacement of marked points obtained from the PIV, the bias of the average displacement from the true displacement, and the standard deviation of the displacements from PIV. According to the ASTM standard (2008), the bias and the standard deviation indicate the accuracy and precision of measurement, respectively. The accuracy and precision were tested along the range of the reference displacement from 0.006 to 0.177 mm. The biases of the PIV displacement range between -0.0024 and 0.0031 mm, while the standard deviations of the PIV displacements range between 0.0022 and 0.0032 mm.

From these accuracy and precision, it is difficult to convince that the PIV displacements are sufficiently exact. However, PIV measures displacements of various points in more detail than a general LVDT with 0.01mm resolution. The elevation of the accuracy and precision is demanded through improvements of hardware settings and analysis algorithms later on.

Table 2. Accuracy and precision of displacement from PIV (mm)

Displacement in Micrometer	Average of PIV displacements	Bias	Standard deviation of PIV displacements
0.006	0.0048	0.0012	0.0023
0.018	0.0155	0.0025	0.0023
0.025	0.0219	0.0031	0.0026
0.043	0.0453	-0.0023	0.0022
0.071	0.0734	-0.0024	0.0023
0.114	0.1125	0.0015	0.0027
0.177	0.1748	0.0022	0.0032

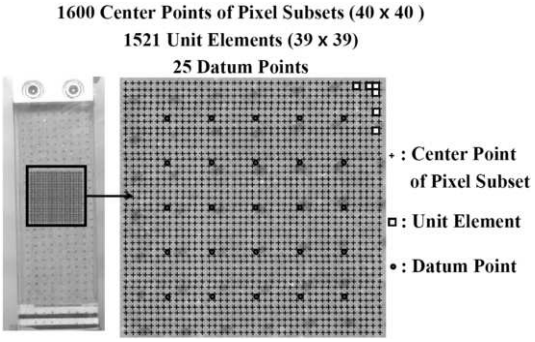

Figure 3. Center points of pixel subsets, unit elements and datum points in analysis area

To avoid the effect of friction, the images were taken only in the middle of the transparent window of the side wall. For PIV, 40 x 40 grid points which serve as centers of pixel subsets were digitally placed on the image, as shown in Figure 3. Each of 1600 pixel subsets consists of 30 x 30 pixels. To make more obvious pattern on the image, we marked additional reference points on the membrane. The PIV displacements were evaluated for two sections of global axial strain increments before failure; 0.00 ~ 0.28 % and 2.32 ~ 2.59 %. The first section of the global axial strain increment corresponds to the initial state of the compressed specimen. At the second section of the global strain, the specimen is about to reach the peak state in the stress-strain curve. Figure 4 plots parts of incremental displacement vectors in the middle of the specimen at two sections of the global strain increment obtained from the PIV.

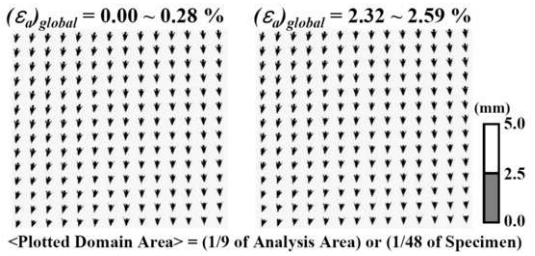

Figure 4 Incremental displacement vectors

4 STATISTICAL RVE

4.1 *Procedure and Method*

To compute the optimum size of the RVE, the deformation moduli among mechanical properties were used. The deformation moduli were computed from the engineering strains, which can be obtained as follows:

(1) For obtaining base data for statistical analysis, 39 x 39 unit elements, each of which consists of 4 neighboring grid points in Figure 3 are organized. The linear displacement field of a unit element is determined based on the least square error. From these calculations, the displacement fields (Δu, Δv) in the plain strain condition are defined at each unit element

(2) Prior to calculating strains at datum points, the local strain increments, Δe^i_{xx}, Δe^i_{yy}, and Δe^i_{xy}, of the *i*-th unit element can be computed by

$$\Delta e^i_{xx} = \frac{\partial u^i}{\partial x}, \quad \Delta e^i_{yy} = \frac{\partial v^i}{\partial y}, \quad \Delta e^i_{xy} = \frac{1}{2}\left(\frac{\partial u^i}{\partial y} + \frac{\partial v^i}{\partial x}\right) \tag{1}$$

(3) To determine datum points, where the increments of engineering strains ($\Delta\varepsilon_{xx}$, $\Delta\varepsilon_{yy}$, and $\Delta\varepsilon_{xy}$) are calculated, 25 equally-spaced points are selected as shown in Figure 3. Various volume sizes together with the number of unit elements for averaging strain increments at datum points are given in Table 3. The increments of volume-averaged strains at 25 datum points are computed as

$$\Delta\varepsilon_{xx} = \frac{\sum_i^N \Delta e^i_{xx}\Delta v^i}{V}, \Delta\varepsilon_{yy} = \frac{\sum_i^N \Delta e^i_{yy}\Delta v^i}{V}, \Delta\varepsilon_{xy} = \frac{\sum_i^N \Delta e^i_{xy}\Delta v^i}{V} \tag{2}$$

where N is the number of unit elements in the analyzed domain V. The value of Δv^i is the volume of the *i*-th unit element. Since this weighting is a constant for all unit elements, Eq. (2) can be rewritten as

$$\Delta\varepsilon_{xx} = \frac{1}{N}\sum_i^N \Delta e^i_{xx}, \quad \Delta\varepsilon_{yy} = \frac{1}{N}\sum_i^N \Delta e^i_{yy}, \quad \Delta\varepsilon_{xy} = \frac{1}{N}\sum_i^N \Delta e^i_{xy} \tag{3}$$

Table 3. Volume sizes and number of unit elements for datum points

Number of Unit Elements	Volume Size(mm)
1 x 1 (1)	0.8 x 0.8
3 x 3 (9)	2.4 x 2.4
5 x 5 (25)	4.0 x 4.0
7 x 7 (49)	5.6 x 5.6
9 x 9 (81)	7.2 x 7.2
11 x 11 (121)	8.8 x 8.8
13 x 13 (169)	10.4 x 10.4
15 x 15 (225)	12.0 x 12.0

(4) To calculate the deformation moduli based on the engineering strains, we introduce the following assumptions:
- The stress field is homogeneous, thus the internal stresses are equal to external tractions on boundaries,
- The cross-anisotropic elasticity can describe the constitutive response of the specimen,
- Three Poisson's ratios of the cross-anisotropic elasticity for Jumunjin sand are evaluated based on preliminary experiments conducted by Ko (2007).

For the plane-strain compression test, the constitutive relation can be described as

$$\begin{aligned}\Delta\varepsilon_{xx} &= -\frac{1}{E_y}\left(\nu_{yx} + \nu_{xx}\nu_{yx}\right)\Delta\sigma_{yy} \\ \Delta\varepsilon_{yy} &= \frac{1}{E_y}\left(1 - \nu_{xy}\nu_{yx}\right)\Delta\sigma_{yy}\end{aligned} \tag{4}$$

where E_y is the Young's modulus in the axial direction, ν_{xy} (ν_{yx}) is the Poisson's ratio of strain in the direction horizontal (axial) to the applied strain in the axial (horizontal) direction, and ν_{xx} is the Poisson's ratio of strain the direction horizontal to the applied strain in orthogonal horizontal direction.

By solving two above equations, the deformation modulus, E_y, can be obtained.

4.2 *Optimum size of the RVE in plane strain compression*

The deformation moduli distributions at each of 25 datum points were computed. Figure 5 shows the distributions of

deformation moduli, E_y, at the global axial strain increments of 0.00 ~ 0.28 and 2.32 ~ 2.59%, respectively. Table 4 summarizes the statistics of the distribution of the deformation moduli for the number of the unit elements used in averaging.

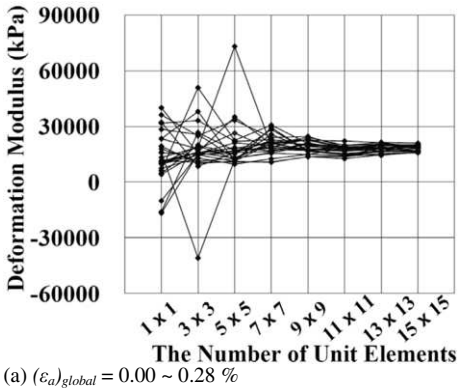

(a) $(\varepsilon_a)_{global}$ = 0.00 ~ 0.28 %

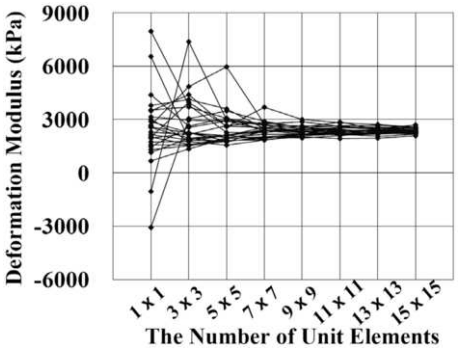

(b) $(\varepsilon_a)_{global}$ = 2.32 ~ 2.59 %

Figure 5. Deformation moduli distributions for various numbers of unit element in averaging.

The minimum RVE size depends on how much we can admit the variance of material properties: The more accuracy in an analysis is required, the less variance of a material property is allowed. Herein, the coefficient of variation (COV), defined as the ratio of the standard deviation to the average, is chosen as the quantitative criteria in determining the minimum RVE size. Duncan (2000) reported that the COVs for the compression index, which could approximate COVs for the deformation modulus used in the study, are ranging from 10 % to 37 %.

In this study, it is assumed that the COV for the deformation modulus do not exceed 20 %. At the initial stage of the plane strain compression, $(\varepsilon_a)_{global}$ = 0.00 ~ 0.28%, the variance among the average deformation modulus at 25 points, represented by the COV, becomes smaller as the number of elements (volume size) increases. This also implies that local heterogeneity in the strain field cannot be properly obtained if the volume for average value is oversized.

To obtain the RVE which has the COV less than 20%, the RVE should be larger than the 9 x 9 elements at $(\varepsilon_a)_{global}$ = 0.00 ~ 0.28%. For $(\varepsilon_a)_{global}$ = 2.32 ~ 2.59%, on the verge of the peak state, the minimum size of the RVE becomes 7 x 7 elements, as shown in Table 4.

Therefore, to represent deformation heterogeneity, the reasonable optimum of the RVE size in plane strain compression before failure is estimated to be 9 x 9, or 7.2 mm x 7.2 mm. For the practical use, the RVE size of Jumunjin sand could be chosen as 13 x 13 D_{50}.

Table 4. Results of deformation moduli distribution

Total Number of Unit Elements	Global Axial Strain 0.00 ~ 0.28 %			Global Axial Strain 2.32 ~ 2.59 %		
	Ave. (kPa)	Std. Dev. (kPa)	COV	Ave. (kPa)	Std. Dev. (kPa)	COV
1 x 1	13557	14487	1.069	2427	2120	0.873
3 x 3	17017	15410	0.906	2777	1387	0.500
5 x 5	19348	13002	0.672	2512	924	0.368
7 x 7	20055	5159	0.257	2400	418	0.174
9 x 9	18773	3104	0.165	2350	256	0.109
11 x 11	17324	2250	0.130	2376	234	0.098
13 x 13	18248	1977	0.108	2344	173	0.074
15 x 15	18346	1520	0.083	2365	158	0.065

5 CONCLUSION

To investigate the optimum RVE size of granular soils, the digital image analysis technique, which generates the displacement field, was used in the plane strain compression experiment. The distributions of the deformation moduli at 25 datum points were analyzed for various volume sizes in averaging. The COV of the deformation moduli distributions was used as criteria to determine the optimum RVE size.

To describe the variance of the deformation moduli within the COV of 20%, the optimum RVE size of Jumunjin sand under the plane strain compression is 7.2 mm x 7.2 mm. To draw general conclusions on the optimum RVE size for various soils, intensive experimental program with digital image processing will be needed.

REFERENCES

Drugan, W. J., and Willis, J. R. 1996. A micromechanics-based nonlocal constitutive equation and estimates of representative volume element size for elastic composites. *Journal of the Mechanics and Physics of Solids*, 44(4), 497-524.

Duncan, J. M. 2000. Factors of safety and reliability in geotechnical engineering. *Journal of Geotechnical and Geoenvironmental Engineering*, 126(4), 307-316.

Grufman, C., and Ellyin, F. 2007. Determining a representative volume element capturing the morphology of fibre reinforced polymer composites. *Composites Science and Technology*, 67(3-4), 766-775.

Kanit, T., Forest, S., Galliet, I., Mounoury, V., and Jeulin, D. 2003. Determination of the size of the representative volume element for random composites: statistical and numerical approach. *International Journal of Solids and Structures*, 40(13-14), 3647-3679.

Ko, Y. J. 2007. Experimental study on the small strain stiffness and nonlinear deformation characteristics of sands. Master thesis, Seoul National Univ.

Kruyt, N. P., and Rothenburg, L. 2001. Statistics of the elastic behaviour of granular materials. *International Journal of Solids and Structures*, 38(28-29), 4879-4899.

Rechenmacher, A. L., and Finno, R. J. 2004. Digital image correlation to evaluate shear banding in dilative sands. *Geotechnical Testing Journal*, 27(1), 13-22.

Trias, D., Costa, J., Turon, A., and Hurtado, J. E. 2006. Determination of the critical size of a statistical representative volume element (SRVE) for carbon reinforced polymers. *Acta Materialia*, 3471-3484.

Wellmann, C., Lillie, C., and Wriggers, P. 2008. Homogenization of granular material modeled by a three-dimensional discrete element method. *Computers and Geotechnics*, 35(3), 394-405.

White, D. J., Take, W. A., and Bolton, M. D. 2003. Soil deformation measurement using particle image velocimetry (PIV) and photogrammetry. *Geotechnique,* 53(7), 619-631.